Evaluation and Projections of Surface Air Temperature over the Tibetan Plateau from CMIP6 and CMIP5: Warming Trend and Uncertainty

Minpei Zhou (zmp0911@hhu.edu.cn)
Hohai University College of Hydrology and Water Resources https://orcid.org/0000-0003-2723-5830
Zhongbo Yu
State Key Laboratory of Hydrology-Water Resources and Hydraulic Engineering
Huanghe Gu
Hohai University College of Hydrology and Water Resources
Qin Ju
Hohai University College of Hydrology and Water Resources
Yiyan Gao
Hohai University College of Hydrology and Water Resources
Lei Wen
Hohai University College of Hydrology and Water Resources
Tangkai Huang
Hohai University College of Hydrology and Water Resources

Research Article

Keywords: CMIP6-CMIP5 comparison, Climate model evaluation, Future climate change, Elevation-dependent warming, Uncertainty in different elevation zones, Tibetan Plateau

Posted Date: March 11th, 2022

DOI: https://doi.org/10.21203/rs.3.rs-1404623/v1

Abstract

This paper compares the historical simulations and future projections of surface air temperature over the Tibetan Plateau of the updated Coupled Model Intercomparison Project phase (CMIP6) and the precedent phase of the project (CMIP5) to quantify differences in the projections under different scenarios. Model evaluation for the historical period (1961-2005) indicates that the multi-model ensemble (MME) mean of CMIP6 outperforms CMIP5 MME in simulating spatial-temporal characteristics of surface air temperature. The temperature changes relative to 1986-2005 are projected in the near-term (2021-2040), mid-term (2041-2060), and long-term (2081-2100) future under Shared Socio-economic Pathway (SSP)2-4.5 and SSP5-8.5 of CMIP6 and Representative Concentration Pathway (RCP)4.5 and RCP8.5 of CMIP5. The projected temperature shows larger increases in the long-term compared with the near-term and mid-term under both SSPs and RCPs. CMIP6 MME projects higher temperature changes and accelerated warming trends relative to CMIP5 MME. Additionally, the temperature increases and warming rates show a significant elevation dependency, especially in the long-term. The uncertainty for future projections is quantified by the square root of error variance (SREV) method. The results record a clear reduction in the uncertainty of CMIP6 temperature relative to CMIP5 primarily concentrated at the elevation zones of over 5,000 m. The analysis of the projected temperature over the Tibetan Plateau is of great significance for policy-makers to make socio-economic adjustments for the future warming. This study is conducive to the credibility of future temperature projections for CMIP6 and enhances our comprehension of the uncertainty of SSP and RCP scenarios.

1. Introduction

In the first two decades of the 21st century (2001–2020), the global surface air temperature was 0.99°C higher than 1850–1900 (IPCC 2021). Global warming has become an accepted fact, particularly at northern high latitudes and high-altitude areas, such as the Rockies Mountains, the Alps, and the Tibetan Plateau(Hansen et al. 2010); (Yao et al. 2012). The Tibetan Plateau (TP), the inland plateau of Asia, is the largest and highest plateau in the world, with a mean altitude exceeding 4,000 m. It is described as the “Water Tower of Asia” because several major rivers originate from the TP, including the Yellow River, the Yangtze River, the Mekong River, and the Brahmaputra River (Yao et al. 2012).

The climate over the TP is complex and has intense sensitivity to climate change, primarily affected by the interaction of the Asian monsoon and the mid-latitude westerlies (Yao et al. 2019). The TP has experienced remarkable warming during the recent decades (Zou et al. 2014; Cai et al. 2017; Duan et al. 2020; Wang et al. 2021). Meteorological datasets indicate that the TP’s warming rate is twice of that observed worldwide in the last 50 years (Duan and Xiao 2015). The strongest warming occurred in the winter months (Du et al. 2004; Chen et al. 2006; Zou et al. 2014; Chen et al. 2016). Growing evidence reveals enhanced warming with elevation (Li et al. 2017) or elevation-dependent warming (Pepin et al. 2015) over the Tibetan Plateau. It is manifested that such inclinations may remain in the future, particularly in winter and spring (Liu et al. 2009; You et al. 2020). The TP has the largest glaciers other than the polar regions, as well as widespread alpine permafrost, snow cover, and lake ice (You et al. 2021). Significant glacier retreating, snowmelt, the degradation of permafrost, desertification, and vegetation change over the TP have been rapidly influenced by the amplified climate warming (Thakuri et al. 2019; Kuang and Jiao 2016; Wang et al. 2017; Gao et al. 2015). Hence, Future warming and its elevation-dependency are of significant impacts on the ecological environment and water resources over the Tibetan Plateau.

Global climate models (GCMs) are crucial tools for climate attribution and projection researches and have been widely applied to reproduce the historical climate and project the potential future climate change. Although climate models have experienced significant evolutions over the past decades, they still fail to capture the dynamics of a local scale process (e.g., cloud feedback, land-use changes, topography) because of their coarse spatial resolutions (Reichler and Kim 2008; Sharma et al. 2018; Gusain et al. 2020). Climate change projections have been reported in various study areas under different emission scenarios from the most frequent GCMs participating in the Coupled Model Intercomparison Project (CMIP) Phase 3/5 (Jia et al. 2019; Fahad et al. 2018; Gu et al. 2015; Chen and Frauenfeld 2014a, 2014b; Maloney et al. 2014; Kharin et al. 2013; Rogelj et al. 2012). Despite the improvements (including terrestrial and marine carbon cycles, dynamic vegetation and etc.) comprised in CMIP5 models (Jia et al. 2019; Fahad et al. 2018; Gu et al. 2015; Chen and Frauenfeld 2014a, 2014b; Maloney et al. 2014; Kharin et al. 2013; Rogelj et al. 2012), CMIP5 models still have pronounced cold biases in simulating surface air temperature over the Tibetan Plateau (Su et al. 2013; Chen and Frauenfeld 2014b).

Currently, the new sixth phase CMIP multi-model datasets developed by different institutions have become available. CMIP6 models display a substantial extension relative to CMIP5, owing to the remarkable changes in CMIP6 dynamical core structure, such as improved spatial and vertical resolutions, revised microphysics parameterizations, advanced deep convective schemes, modified ocean-ice models (Eyring et al. 2016; Gerber and Manzini 2016). The deficiencies identified in CMIP5 models are expected to be remedied or

even overcome, notably in the TP. Shared Socioeconomic Pathway (SSP) scenarios are advocated for CMIP6 future projections, in place of the Representative Concentration Pathway (RCP) scenarios of CMIP5 (O'Neill et al. 2016; Taylor et al. 2012). SSP scenarios clearly describe and quantify both emission pathways and land-use changes (Riahi et al. 2017). Therefore, SSPs provide a more specific explanation of future socio-economic evolution and offer more realistic future climate projections.

Several recent studies compare the simulations and outputs of CMIP5 and CMIP6 (Tokarska et al. 2020; Su et al. 2021; Wang et al. 2021; Tebaldi et al. 2020; Chen et al. 2021). The performance of CMIP5 and CMIP6 models has been found to be site-specific and irregular (Song et al. 2021), and CMIP6 models exhibit better capabilities in historical climate simulations (Zhu et al. 2021; Zhu and Yang 2020; Lun et al. 2021; Zamani et al. 2020). The above studies primarily focused on the evaluation and comparison of the performance of CMIP5 and CMIP6 models in reproducing the historical climate. However, little achievements have been revealed for the future projections of surface air temperature over the TP under different emission scenarios from CMIP5 and CMIP6 models.

GCMs are widely used for climate projections, but are subjected to high uncertainty owing to standard errors mainly resulting from the model structures, scenarios and ensembles (Hawkins and Sutton 2011; Woldemeskel et al. 2014; Yip et al. 2011; Bennett et al. 2012). Several studies have demonstrated that models are the main source of total uncertainty, followed by emission scenarios (Jobst et al. 2018; You et al. 2021). Square Root of Error Variance (SREV) method proposed by Woldemeskel et al. (2012) can quantify such uncertainties in space and time. Woldemeskel et al. (2016) used the SREV to quantify and compare uncertainty in climate projections using 6 CMIP3 and 13 CMIP5 models. Kim et al. (2020) adopted the SREV to access the uncertainty in extreme daily precipitation from 45 projections of CMIP5. Eghdamirad et al. (2016) utilized the SREV to quantify the contribution of different sources of uncertainty in upper air climate variables. These studies manifested that uncertainty estimates using the SREV method have a high confidence level.

This study uses CMIP5 and CMIP6 experiments to perform an assessment of the capability of the models to simulate the surface air temperature over the TP and to quantify differences in their projections of future temperature changes for the near-term (2021–2040), mid-term (2061–2080) and long-term (2081–2100) future from spatio-temporal and elevational perspectives. The moderate and high scenarios (SSP2-4.5/SSP5-8.5 for CMIP6 and RCP4.5/RCP8.5 for CMIP5) are mainly focused on in this study. The key issues that we emphasize are as follows. (1) How do the CMIP6 models perform in simulating the historical surface air temperature over the Tibetan Plateau, whether CMIP6 models exhibit improvements over their CMIP5 predecessors? (2) What are the differences between CMIP5 and CMIP6 in the possible changes of the projected warming pattern over the Tibetan Plateau? (3) Does the Tibetan Plateau’s warming show dependency with elevation in the future projections? (4) For different elevation zones, are there any differences between CMIP5 and CMIP6 in uncertain estimates of surface air temperature over the Tibetan Plateau? This study can contribute to adjusting adaptive measures based upon RCP scenarios for the future natural ecosystem.

2. Study Area, Data, And Methods

2.1 Study area

The study area locates in East Asia, limited to the plateau extending between 23°N-40°N and 73°E-106°E, which includes the main part of the Tibetan Plateau within the boundary of China (the black line) (Fig. 1). Hereafter ‘TP’ refers to the range within these borders (the red line).

Table 1
Information of the GCMs used in this study

Modelling Centres	CMIP5 Models	Resolution(lat×lon)	CMIP6 Models	Resolution(lat ×lon)
ACCESS (Australia)	ACCESS1-0	1.25°×1.875°	ACCESS-CM2	1.25°×1.875°
ACCESS (Australia)	ACCESS1-3	1.25°×1.875°	ACCESS-ESM1-5	1.25°×1.875°
BCC (China)	BCC-CSM1-1-m	1.1215°×1.125°	BCC-CSM2-MR	1.1215°×1.125°
NCAR (USA)	CESM1-BGC	0.9424°×1.25°	CESM2	0.9424°×1.25°
CMCC (Italy)	CMCC-CM	0.75°×0.75°	CMCC-CM2-SR5	0.9424°×1.25°
FIO (China)	FIO-ESM	2.7906°×2.8215°	FIO-ESM-2-0	0.9424°×1.25°
GFDL (USA)	GFDL-ESM2G	2.0225°×2.5°	GFDL-ESM4	1°×1.25°
INM (Russia)	INMCM4	1.5°×2°	INM-CM4-8	1.5°×2°
CCSR (Japan)	MIROC5	1.4005°×1.4063°	MIROC6	1.4005°×1.4063°
MPI (Germany)	MPI-ESM-LR	1.8653°×1.875°	MPI-ESM1-2-HR	0.9272°×0.9375°
MPI (Germany)	MPI-ESM-MR	1.8653°×1.875°	MPI-ESM1-2-LR	1.8653°×1.875°
MRI (Japan)	MRI-CGCM3	1.1215°×1.125°	MRI-ESM2-0	1.1215°×1.125°
NCC (Norway)	NorESM1-ME	1.8947°×2.5°	NorESM2-LM	1.8947°×2.5°
NCC (Norway)	NorESM1-M	1.8947°×2.5°	NorESM2-MM	1.8947°×2.5°

2.2 Data

Simulations are evaluated with the observed surface (2m) monthly air temperature data provided by the National Meteorological Information Center (China monthly gridded surface air temperature (Version 2.0), (Shen et al. 2010)), with a spatial resolution of 0.5°×0.5°. The gridded temperature is based on observations from more than 2400 national meteorological stations and spatially interpolated using the Thin Plate Spline (TPS). The dataset has been widely applied in climate change research both for the entire country and the TP (Yang et al. 2021; Zhao et al. 2022; Jin et al. 2013; Gao et al. 2017; Gao et al. 2020).

This study is based on a comparison between 14 GCMs from CMIP6 and an equal number of models available from CMIP5 that belong to the same institutions, to evaluate possible improvements in the representation of regional surface air temperature and detect the changes for SSP scenarios (Prasanna et al. 2020; Song et al. 2020). The names, modeling centers, and resolutions of the analyzed models are presented in Table 1. SSP scenarios can estimate future energy and land-use changes based upon adaptation and mitigation intensity levels, SSP1-2.6, SSP2-4.5, SSP4-6.0, and SSP5-8.5 (O'Neill et al. 2016). The SSP2-4.5 scenario is a combination of a moderate socio-economic development path (i.e., SSP2) with the medium-low radiation forcing, peaking at 4.5 W/m^2 by 2100. The SSP5-8.5 scenario is a combination of a high socio-economic developmental path (i.e., SSP5) with strong radiative forcing, peaking at 8.5 W/m^2 by 2100 (Riahi et al. 2017; O'Neill et al. 2016). In this study, two SPP scenarios (SSP2-4.5 and 5-8.5) and their equivalent RCP scenarios (RCP4.5 and 8.5) are used. To facilitate GCMs intercomparison, the 28 GCMs are bilinearly interpolated to a common grid of 0.5°×0.5°, consistent with the resolution of the gridded-observation datasets.

The multi-model ensemble (MME) mean reduces inter-GCM uncertainties on account of their diversities in model structures and physics. To further evaluate the seasonal performance of GCMs, the annual, summer (June-August, JJA) and winter (December-February, DJF) surface air temperature characteristics are discussed separately. In this study, we compare the spatial and temporal patterns of simulated temperature with the observations during 1961–2005. Simulation outputs under RCP4.5/RCP8.5 and SSP2-4.5/SSP5-8.5 are selected during 2006–2100 and 2015–2100, respectively. Three projection periods, defined as near-term (2021–2040), mid-term (2041–2060) and long-term (2081–2100) future, are used for further research.

2.3 Analysis methods

A Taylor Diagram (Taylor 2001) is constructed to statistically quantify the correspondence between the observations and the individual GCM and MME simulations in terms of three statistics (correlation coefficient, root-mean-square error, and the ratio of standard

deviations). The higher the correlation coefficient, the smaller the root-mean-square error, and the smaller ratio of standard deviation indicate the better simulations.

Uncertainty in the climate change projections can be divided into three main sources: the model structure, emission scenario, and natural variability (Woldemeskel et al. 2012, 2016). In this study, only one run of each GCM is considered, identified as r1i1p1 and r1i1p1f1 for CMIP5 and CMIP6, respectively. Thus, the uncertainty of the climate projections primarily arises from model and scenario uncertainty. The square root of error variance (SREV) proposed by (Woldemeskel et al. 2016, 2012) is employed to identify these two sources of uncertainty. Here we provide a brief illustration of the SREV method.

1. Firstly, the GCM data are converted to percentiles at each grid cell to establish deviations across each simulation in percentile space.

2. SREV for a percentile of interest is estimated as standard deviations for each souce of uncertainty. The model (M) and senario (S) uncertaionties at each pencentile (p), demostrated as $SREV_p^M$ and $SREV_p^S$ respectively, are calculated by

$$SREV_p^M = \left[\frac{1}{n_S\left(n_M - 1\right)} \sum_{j=1}^{n_S} \sum_{i=1}^{n_M} \left(x_{i,j,p} - \bar{x}_{j,p} \right)^2 \right]^{0.5} \quad (1)$$

$$SREV_p^S = \left[\frac{1}{n_M\left(n_S - 1\right)} \sum_{i=1}^{n_M} \sum_{j=1}^{n_S} \left(x_{i,j,p} - \bar{x}_{i,p} \right)^2 \right]^{0.5} \quad (2)$$

where n_M and n_S represent the number of models and senarios, respectively. $x_{i,j,p}$ is the pth percentile of a projection for the ith model and jth senario. The means of values for all models and senarios at the pth percentile are denoted as $\bar{x}_{j,p}$ and $\bar{x}_{i,p}$, respectively.

3. The SREV method is based on the assumption that the two sources of uncertainty are independent of each other, i.e. there is no interaction between them. Thus, the total uncertainty $SREV_p^T$ is

$$SREV_p^T = \left[\left(SREV_p^M\right)^2 + \left(SREV_p^S\right)^2 \right]^{0.5} \quad (3)$$

3 Results

3.1 Evaluation of historical temperature from CMIP5/6 models

Figure 2 shows the annual, summer (June to August, JJA)and winter (December to February, DJF) surface air temperature variations from the observations (the first line), the multi-model ensemble (MME) mean of 14 CMIP6 models (the second line) and the corresponding CMIP5 models (the third line), as well as their temperature bias (the fourth and fifth lines) over the TP during 1961–2005.

In general, similar spatial patterns can be found between the observation and CMIP5/6 MME, with a decreasing gradient from northeast to southwest. In addition, both the CMIP6 and CMIP5 MMEs can identify the effects of topography on the surface air temperature that the cold center appears in the northwestern TP with an elevation exceeding 5,000 m, and the warm center appears in the southern edge of the TP and the Qaidam Basin where the elevation is relatively lower (Figs. 2a-i). There is a general underestimation of annual and winter surface air temperature simulations, with larger biases in the northwestern TP. In addition, the warm bias is concentrated on the eastern and northern edges of the TP. The annual and winter surface mean temperature biases are − 0.11/-1.38 ℃ and − 1.13/-2.78 ℃ respectively in CMIP6/5. In summer, although CMIP6 MME shows a positive bias over the TP (0.57 ℃) and the absolute value appears to be larger, its cold bias in the northwest is smaller compared with CMIP5 MME (Fig. 2k). In contrast, the cold bias and warm bias of

CMIP5 are both large and cancel each other out, resulting in a small overall bias (-0.13 ℃) (Fig. 2n). Hence the CMIP6 MME reasonably reduces the cold bias, and the simulation value is much closer to the observation than CMIP5.

Figure 3 exhibits the spatial variability statistics of each model and their MMEs for CMIP6 and CMIP5 sets in reproducing the annual, summer, and winter surface mean temperature based on the Taylor Diagrams (Taylor. 2001). Most (ten of fourteen) of the CMIP6 models simulate a similar or larger correlation coefficient (R), and most (eleven of fourteen) of the CMIP6 models simulate a smaller root-mean-square error (RMSE), relative to the corresponding CMIP5 models in annual temperature simulations. Additionally, the CMIP6 MME is superior to CMIP5 MME in capturing the spatial variability with the larger spatial correlation coefficient and the lower RMSE in reproducing the annual, summer, and winter surface air temperature over the TP.

Figure 4 reveals that the annual mean warming rate of the TP is 0.34 ℃/decade in the observation during 1961–2005, with more significant warming in winter (0.41 ℃/decade) than in summer (0.30 ℃/decade). Both the MMEs of CMIP6 and CMIP5 GCMs have capability in capturing the observed annual, summer, and winter warming, but with lower warming rates. However, the warming trends simulated by CMIP6 are relatively closer to the observed trends than that of CMIP5. To summarize, CMIP6 models have enhanced capability in reproducing the historical surface air temperature over the TP.

3.2 Projected future temperature changes from CMIP5/6 models

3.2.1 Spatiotemporal variations in temperature changes

Time series of annual, summer, and winter surface mean temperature projections under RCP4.5/8.5 and SSP2-4.5/5-8.5 scenarios from the MMEs of CMIP5 and CMIP6 respectively are shown in Fig. 4. The spatial distribution and trends of annual, summer, and winter surface air temperature from the MMEs of CMIP5 and CMIP6 GCMs in the near-, mid- and long-term under RCP4.5/8.5 and SSP2-4.5/5-8.5 scenarios are presented in Figs. 5,6, respectively. The projected changes in annual, summer and winter surface air temperature and detailed trends for the same scenarios are also summarized in Table 2 and Table 3, respectively.

Table 2
Projected changes and differences (℃) in annual, summer and winter surface mean temperature relative to 1986–2005 period from the MMEs of CMIP5/6 under RCP4.5, RCP8.5, SSP2-4.5 and SSP5-8.5 scenarios in the near-term (2021–2040), mid-term (2041–2060) and long-term (2081–2100)

Change	Annual				Summer				Winter			
	RCP4.5	RCP8.5	SSP2-4.5	SSP5-8.5	RCP4.5	RCP8.5	SSP2-4.5	SSP5-8.5	RCP4.5	RCP8.5	SSP2-4.5	SSP5-8.5
Near-term	1.15	1.3	1.29	1.41	1.04	1.17	1.22	1.39	1.23	1.4	1.42	1.58
Mid-term	1.8	2.42	2	2.52	1.63	2.19	1.88	2.46	1.95	2.59	2.23	2.77
Long-term	2.44	5.03	2.89	5.36	2.26	4.60	2.72	5.01	2.63	5.48	3.24	5.92
Difference	**Annual**				**Summer**				**Winter**			
	(SSP2-4.5)-(RCP4.5)		(SSP5-8.5)-(RCP8.5)		(SSP2-4.5)-(RCP4.5)		(SSP5-8.5)-(RCP8.5)		(SSP2-4.5)-(RCP4.5)		(SSP5-8.5)-(RCP8.5)	
Near-term	0.14		0.11		0.18		0.22		0.19		0.18	
Mid-term	0.2		0.1		0.25		0.27		0.28		0.18	
Long-term	0.45		0.33		0.46		0.41		0.61		0.44	

Table 3
As in Table 2, but for warming trends of surface mean temperature (℃/decade)

Trend	Annual				Summer				Winter			
	RCP4.5	RCP8.5	SSP2-4.5	SSP5-8.5	RCP4.5	RCP8.5	SSP2-4.5	SSP5-8.5	RCP4.5	RCP8.5	SSP2-4.5	SSP5-8.5
Near-term	0.35	0.35	0.31	0.5	0.31	0.37	0.32	0.45	0.4	0.27	0.36	0.54
Mid-term	0.26	0.63	0.29	0.61	0.29	0.48	0.31	0.61	0.25	0.82	0.36	0.67
Long-term	0.02	0.68	0.18	0.74	0.07	0.57	0.11	0.68	-0.05	0.88	0.21	0.83
Difference	**Annual**				**Summer**				**Winter**			
	(SSP2-4.5)-(RCP4.5)		**(SSP5-8.5)-(RCP8.5)**		**(SSP2-4.5)-(RCP4.5)**		**(SSP5-8.5)-(RCP8.5)**		**(SSP2-4.5)-(RCP4.5)**		**(SSP5-8.5)-(RCP8.5)**	
Near-term	-0.04		0.15		0.01		0.08		-0.04		0.27	
Mid-term	0.03		-0.02		0.02		0.13		0.11		-0.15	
Long-term	0.16		0.06		0.04		0.11		0.26		-0.05	

The time series in Fig. 4 indicates little differences in the surface mean temperature change between SSP and RCP scenarios for the near- and mid-term, but there are extensive differences in the long-term. The projected temperature increases are particularly rapid for SSP5-8.5 and RCP8.5 compared with two moderate scenarios and this sensitivity is enhanced further for winter. Relative to reference period 1986–2005, the increase in annual surface mean temperature by the end of the 21st century projected by the MME of CMIP6 are 2.92 ℃ and 6 ℃ under SSP2-4.5 and SSP5-8.5, respectively. Compared with the result projected by CMIP6, the MMEs of CMIP5 projected a smaller increase under RCP4.5 and RCP8.5 (2.57 ℃ and 5.78 ℃, respectively).

Under the SSP2-4.5 scenario, the annual surface mean temperature of the CMIP6 MME over the TP projects significant warming relative to the 1986–2005 period in the near-and mid-term, and then the warming rate slows down in the long-term. The temperature increase will reach 1.29/2.01/2.89 ℃, with an annual mean warming trend of 0.31/0.29/0.18 ℃/decade in the near-/mid-/long-term, respectively (Figs. 5,6). Under the SSP5-8.5 scenario, the annual surface mean temperature of the CMIP6 MME increases by 2.52 ℃ in the mid-term, and breaches 5 ℃ in the long-term, with annual mean warming rates of 0.61 and 0.74 ℃/decade, respectively. Spatial projections under both RCP and SSP scenarios are proved to be highly consistent. The annual surface mean temperature over the TP is projected to increase and exhibit positive trends in the near-, mid-, and long-term (Figs. 5,6 and Table 2 and Table 3). Additionally, the annual surface mean temperature under SSP scenarios is characterized with higher magnitudes of increase and warming rate than those under RCP scenarios (Table 2 and Table 3), except for the warming rate under SSP2-4.5 in the near-term and SSP5-8.5 in the mid-term. Consequently, compared with the RCP scenarios, the SSP scenarios project greater variability and more extremes in temperature. The warming patterns exhibit consistency for the entire TP, with larger temperature changes in the long-term than in the near- and mid-term and a higher magnitude of increase and a more rapid warming rate under high scenarios than those projected under moderate scenarios. The coldest region of the TP, the Qiangtang plateau, exhibits a particularly rapid warming rate than the rest of the TP. At the seasonal scale, the result reveals that the magnitudes of increase and warming trends in the freezing season (winter) are higher than those in the melting season (summer), except for the warming rate in winter under RCP4.5 in the long-term.

3.2.2 Elevation-dependent warming in the future

The projected annual, summer and winter surface air temperature changes (relative to 1986–2005 period) and warming trends from the two CMIP MMEs under RCP/SSP scenarios are compared from the perspective of different elevation zones (Figs. 7,8). The means of annual surface air temperature changes and warming trends over individual elevation zones are shown in Table 4 and Table 5.

Table 4
Means of annual surface air temperature changes (°C) over individual elevation zones

Elevation (m)		< 2000	2000–3000	3000–4000	4000–5000	> 5000
Near-term	RCP4.5	1.01	1.08	1.1	1.16	1.2
	SSP2-4.5	1.02	1.24	1.25	1.31	1.34
	RCP8.5	1.08	1.22	1.24	1.32	1.36
	SSP5-8.5	1.11	1.38	1.37	1.42	1.47
Mid-term	RCP4.5	1.55	1.69	1.71	1.82	1.9
	SSP2-4.5	1.65	1.94	1.94	2.02	2.06
	RCP8.5	2.03	2.25	2.29	2.46	2.54
	SSP5-8.5	2.1	2.45	2.45	2.56	2.6
Long-term	RCP4.5	2.14	2.3	2.33	2.48	2.56
	SSP2-4.5	2.49	2.82	2.81	2.93	2.98
	RCP8.5	4.33	4.76	4.81	5.1	5.26
	SSP5-8.5	4.64	5.21	5.21	5.41	5.52

Table 5
As in Table 4, but for warming trends (°C/decade)

Elevation (m)		< 2000	2000–3000	3000–4000	4000–5000	> 5000
Near-term	RCP4.5	0.33	0.35	0.36	0.35	0.34
	SSP2-4.5	0.30	0.35	0.35	0.31	0.28
	RCP8.5	0.34	0.32	0.33	0.36	0.36
	SSP5-8.5	0.41	0.47	0.48	0.51	0.50
Mid-term	RCP4.5	0.26	0.30	0.28	0.25	0.26
	SSP2-4.5	0.31	0.31	0.31	0.29	0.28
	RCP8.5	0.59	0.63	0.62	0.63	0.63
	SSP5-8.5	0.54	0.62	0.60	0.61	0.61
Long-term	RCP4.5	0	0	0.01	0.03	0.04
	SSP2-4.5	0.11	0.13	0.14	0.19	0.21
	RCP8.5	0.60	0.64	0.63	0.69	0.71
	SSP5-8.5	0.67	0.74	0.72	0.74	0.79

Under SSP scenarios, the annual temperature change increases with a rise in elevation for three time slices (Fig. 7 (left column)). The average temperature increases at the elevation of less than 2,000 m are much lower than those at other elevation zones, especially in the long-term. Notably, the maximum average temperature increase appears at the elevation zone exceeding 5,000 m, which is a bit higher than the average temperature increase of the whole TP (Table 4). In terms of the projected differences between RCP and SSP scenarios, the magnitudes of temperature increase under SSP scenarios are higher than those under RCP scenarios, and more visible differences occur at the elevation of 2,000–3,000 m and in the long-term. Furthermore, values projected under SSP scenarios exhibit a wider range of temperature change than those under RCP scenarios, which indicates that CMIP6 considers the complexity and heterogeneity inherent in the TP. At the seasonal scale, the difference of temperature increases between winter and summer mainly reflects in the high-altitude areas above 4,000 m, which is enhanced under SSP scenarios.

As shown in Fig. 8 (left column), under SSP2-4.5 in the near-term and mid-term, the warming rates of annual surface air temperature first increase as the elevation raises until 4,000 m and then decline as the elevation continues to raise over 5,000 m. The warming rate in the long-term increases with a rise in elevation and it is lower as compared with those in the near- and mid-term. The means of the warming

rates at the elevation of 4,000–5,000 m and more than 5,000 m in the long-term are 0.19 and 0.21 ℃/decade, respectively. Similar change characteristics in warming rates can be found under RCP4.5. However, the trend magnitude under RCP4.5 is a bit higher in the near-term, and lower in the mid-term and long-term relative to SSP2-4.5. Even some negative values appear in the long-term at different elevation zones. Under SSP5-8.5, the warming rates generally increase as the elevation raises over 5,000 m for three time slices, and the magnitude of the warming rate is higher than that under SSP2-4.5. The result reveals that the elevation-dependency of warming can expand to higher elevation when encountering enhanced warming from higher emission scenarios. Contrary to the moderate scenarios, the trend magnitude is higher in the long-term as compared with the other two periods. The means of the warming rate at the elevation of 4,000–5,000 m and more than 5,000 m in the long-term are 0.72 and 0.79 ℃/decade, respectively. The trend magnitude under RCP8.5 is a bit higher in the mid-term and significantly lower in the near- and long-term than that under SSP5-8.5, especially at an elevation over 5,000 m (Table 5). At the seasonal scale, under both high emission scenarios, the difference between winter and summer warming rates in the near-and mid-term is reinforced in the high-altitude areas above 4,000 m relative to other areas of the TP, while SSP2-4.5 of CMIP6 still exhibits the amplification of high altitude warming in the long-term.

3.3 Spatial and elevational uncertainties analysis of CMIP5/6 models

The uncertainties of climate change projections can be divided into three sources: the model structure, emission scenario, and natural variability. In this study, only one run (r1i1p1 for CMIP5 and r1i1p1f1 for CMIP6) of each GCM is considered. Consequently, the contributions of model structure and emission scenario to total uncertainty in the annual, summer, and winter temperature projections are analysed in this section.

Figure. 9 presents the spatial variations of temperature uncertainty from CMIP5 and CMIP6 models for the three time slices. The results reveal that the uncertainty estimates of CMIP5 and CMIP6 both exhibit conspicuous spatial variability, with the maximum values generally obtained in the northwestern TP, where the temperature is relatively colder. The model uncertainty of annual surface mean temperature projections in CMIP6 remains somewhat constant for all regions in the near-, mid-, and long-term, with the unchanging dominance of the contributions (reaching up to more than 80% in the near-term). While as time progresses, an increasing trend regarding scenario uncertainty in the long-term is observed, with the relative percent contribution reaching up to 46%. Comparison of uncertainty estimates from CMIP5 and CMIP6 indicates that remarkable reduction in uncertainty is estimated in CMIP6, which is mainly focused on the model uncertainty in the northwestern and central-eastern TP.

Furthermore, a comparison of CMIP5 and CMIP6 uncertainty estimates is conducted from the perspective of different elevation zones (Figs. 10,11,12). Uncertainty of grids with elevation above 5,000 m is clearly larger than that of the regional average for the three time periods. Relative to CMIP5, there is a general reduction in the total uncertainty of annual surface mean temperature projections in CMIP6 at five elevation zones during three time periods. This phenomenon is chiefly on account of the reduction of model uncertainty, which is more conspicuous in the low-altitude area below 2,000 m and the high-altitude area above 5,000 m. Scenario uncertainty also presents a reduction in CMIP6 projections throughout the three time slices as compared with CMIP5, particularly in the high-altitude region above 5,000 m. The uncertainty of temperature projections presents notable differences between summer and winter, with generally larger uncertainty in winter than in summer (Figs. 11,12). However, the fraction of model uncertainty is similar between seasons and almost constant through time. In summer, there is an amelioration of the uncertainty for CMIP6 in the near-term but a slight deterioration in areas with an elevation of over 4,000 m in the mid- and long-term compared with CMIP5. Meanwhile, the reduction in uncertainty estimates for CMIP6 in winter is marvelous at five elevation zones, most notably in the near- and mid-term. It is concluded that CMIP6 is more reliable compared with CMIP5 in temperature projections over the Tibetan Plateau, including high-altitude areas.

4 Discussion

In this study, we evaluate and compare the ability of 14 GCMs in CMIP5 and 14 corresponding GCMs in CMIP6 in reproducing the spatial-temporal surface mean temperature characteristics by comparing with the observations during 1961–2005. CMIP6 still underestimates the surface mean temperature with a general cold bias over the TP, similar to earlier results from previous generations of CMIP (Su et al. 2013; Chen and Frauenfeld 2014b). Due to their relatively coarse spatial resolution, global climate models cannot portray the complex underlying surface variations of the plateau, which may be responsible for the cold biases (IPCC 2013) (Gao et al. 2008; Kim et al. 2008). On the other hand, the cold biases are pronounced in the freezing season and the western plateau, where there is greater snow coverage. This feature reveals the diverse models suffer from a common failure to represent snow-ice albedo feedback over complex terrain, which may lead to the reduction of the warming magnitudes (Taylor et al. 2012; Ji and Kang 2013; Kang et al. 2019; You et al. 2019). Meanwhile, it is suggested that the cold biases in the TP are probably attributable to model deficiencies in handling the cloud feedback processes, resulting in insufficient plateau heating (Zhou et al. 2017; Zhou and Yu 2006). However,

quantification of the attribution accounting for the biases requires more detailed diagnoses. Although the bias still occurs in the simulations of surface air temperature and its temporal trends in CMIP6 over the TP, this study reveals that the CMIP6 models show better performance than CMIP5 models. Higher model resolution is a crucial step in further improving the confidence of simulations (Zhou 2021). Hence, compared with the CMIP5 models, the improvements in physical process (e.g., sea–air fluxes, ocean mixing, and cloud physical processes) along with the higher spatial resolution in CMIP6 may be responsible for the reinforced simulation capability of the climate models (Wu et al. 2021; Watterson 2015; Su et al. 2021; Zhou et al. 2020; Eyring et al. 2016).

Our diagnosis suggests that both CMIP5 and CMIP6 show consistent warming over the TP in the 21st century and the warming projected in CMIP6 indicate a general amplification relative to CMIP5. The differences of projections between CMIP5 and CMIP6 are primarily owing to the upgrading of climate models and future emission scenarios (O'Neill et al. 2016). The evolution from RCP to SSP manifests that the scientific institutions enhance the climate change topics from a purely physical issue to the socio-economic realm of human society, including mitigation and adaptation. However, it is pointed that the projected differences of surface air temperature between CMIP5 and CMIP6 are mainly ascribed to the upgrading of physical models and the change of their emission scenarios is small and basically negligible (Zhu et al. 2021).

Our analysis of spatio-temporal and elevational changes in surface air temperature from CMIP6 models reveals that rapid warming will continue over the TP in the near-term, mid-term and long-term future. Studies manifest that the accelerated warming over the TP may result from absorbed energy through the snow–albedo feedback and cloud–radiation interactions(Duan and Xiao 2015; Liu and Chen 2000). Changes in land use, atmospheric circulation and surface water vapors are all likely responsible for the warming, particularly for winter warming over the TP (Rangwala et al. 2009; Song et al. 2021). Additionally, snow–albedo feed-backs and solar radiations may contribute to the elevation-dependent warming over the TP (Guo et al. 2016; Zhang et al. 2003; You et al. 2020). As the snow line retreats to higher altitudes under the general climate warming, the surface absorbs more solar radiation, which thus leads to amplified warming at higher altitudes. The warming results in more snow-melting and snow line rise and then forms positive feedback (Yao et al. 2019; Guo et al. 2021). Current demonstrations for accelerated warming and noteworthy elevation-dependency warming mainly come from in situ data below 5,000 m (Ahmed et al. 2020; Guo et al. 2016; You et al. 2020; Guo et al. 2021). However, due to a lack of adequate observations above 5,000 m where glaciers and snow are largely covered, how the air temperatures did, and will, change is still unknown. Hence, the future work is to investigate how will surface air temperature changes at high altitudes and its driving mechanisms.

In this study, the uncertainty resulting from model is the main contributor to the total uncertainty over the TP, similar to the previous studies by (You et al. 2021) and (Gu et al. 2018), which adopt the method proposed by (Gu et al. 2018). Although scenario uncertainty increases during 2081–2100, the dominance of model uncertainty remains the same throughout the 21st century. However, (Hawkins and Sutton 2011) demonstrate that the percentage contribution from scenario uncertainty becomes larger than model uncertainty in temperature projection after about 2050. This diversity of the results may be due to different methods utilized. In our study, uncertainty calculations are identified by concerning about a specific quantile, while previous studies estimate uncertainty for temporal mean of the variable. In addition to spatial uncertainty distributions of temperature projection, our study estimates the uncertainty for grids at different elevation zones. Uncertainty is found to be notably larger in areas with an elevation exceeding 5,000 m in the TP during the future three time slices. These areas encounter relatively colder temperatures, which could result in larger uncertainty.

5 Conclusion

In this study, historical simulations and future projections of annual, summer, and winter surface air temperature outcomes over the TP are compared from the spatial, temporal, and elevational perspectives using 14 models available in both CMIP5 and CMIP6. Two corresponding scenarios RCP4.5/8.5 and SSP2-4.5/5-8.5 are adopted to compare future projections during three future periods: the near-term (2021–2040), mid-term (2041–2060), and long-term (2081–2100). Along with the historical simulations and the trend analysis, this study quantifies and compares the contributions of the model and scenario to the total uncertainty using the square root of error variance (SREV) method in CMIP5 and CMIP6 projections.

For the historical simulation during 1961–2005, both CMIP5 and CMIP6 MMEs underestimate the observed temperature and its warming rate over the TP, particularly in the freezing season. Meanwhile, CMIP6 MME reduces the cold bias in the northwestern TP and the warming rates simulated in CMIP6 are relatively closer to the observed trends. CMIP6 MME shows higher reproducibility of spatial-temporal distribution characteristics of surface mean temperature over the TP compared with CMIP5 MME.

CMIP6 MME indicates consistent warming (with reference to 1986–2005) over the entire domain in the twenty-first century, and seasonal temperature increases drastically in freezing months. The projected temperature shows larger increases in the long-term compared with the near-term and mid-term. The temperature increases projected in CMIP6 are larger than those in CMIP5 and higher emissions always correspond to stronger warming in the mid-term and long-term. In addition, the projected warming rate of annual mean temperature under SSP2-4.5 is similar to that under RCP4.5 in the near-term and mid-term, but larger than that under RCP4.5 in the long-term; the warming rate under SSP5-8.5 is larger than that under RCP8.5 in the near-term but similar to that under RCP8.5 in the mid-term and long-term. The projected warming trend in winter is characterized by generally higher rates than in summer, suggesting that the cold season is more sensitive to future climate warming.

Furthermore, the magnitude of annual temperature change increases with a rise in elevation under both RCP and SSP scenarios, and CMIP6 MME projects much larger values and wider ranges. The average temperature change at the elevation zone exceeding 5,000 m is a bit higher than the average temperature increase of the whole TP. The trend magnitude under SSP2-4.5 is a bit lower in the near-term, and higher in the mid-term and long-term relative to RCP4.5. And the trend magnitude under SSP5-8.5 is a bit higher in the mid-term and significantly lower in the near-term and long-term than that under RCP8.5, especially at an elevation over 5,000 m. Accelerated warming rates at higher elevations (over 4,000 m) in the TP in the 21st century and the elevation-dependency of warming is projected to strengthen by the end of the 21st century under a high-emission scenario. At the seasonal scale, the warming pattern of winter reveals an amplification relative to summer, and the difference of mainly reflects in the high-altitude areas above 4,000 m.

Uncertainty estimates suggest that a significant reduction in uncertainty is obtained in CMIP6 temperature projections relative to those in CMIP5. The model uncertainty is the dominant contributor (more than 80% in the near-term) and remains somewhat constant in the temperature projections in CMIP6. While as time progresses, the scenario uncertainty increases in the long-term (reaching up to 40%). The uncertainty is relatively larger in colder areas at higher altitudes and in winter, and the reduction of the uncertainty in CMIP6 is mainly due to the visible melioration of model uncertainty in high-altitude areas over 5,000 m. Better performance in the uncertainty can reinforce credibility of the CMIP6 models in future temperature projections. Further uncertainty analysis should be included more available climate models.

For continued study, more attention should be paid to the selection of appropriate GCMs for climate change assessments and ensemble modelling of multiple downscaling to obtain more reliable high-resolution model data and project future climatology of the Tibetan Plateau under different emission scenarios, which will have socio-economic implications for dealing with future climate change.

Declarations

Declaration of Competing Interest

We have no competing financial interests or personal relationships that could have appeared to influence the work reported in this paper.

Acknowledgements This work was supported by the National Key R&D Program of China(Grant No. 2021YFC3201104), the National Key R&D Program of China(Grant No. 2016YFC0402710), National Natural Science Foundation of China (Grant No. 51539003, 41761134090) and the Special Fund of State Key Laboratory of Hydrology-Water Resources and Hydraulic Engineering (Grant No. 520004412, 521013122). We express our sincere thanks to the National Meteorological Information Center and National Tibetan Plateau Data Center for providing the observed temperature data and the TP boundary, respectively. The observation datasets are available at http://data.cma.cn/ and the TP boundary dataset is provided by http://data.tpdc.ac.cn/zh-hans/data/61701a2b-31e5-41bf-b0a3-607c2a9bd3b3/.

References

1. Ahmed N, Wang G, Oluwafemi A et al (2020) Temperature trends and elevation dependent warming during 1965–2014 in headwaters of Yangtze River, Qinghai Tibetan Plateau. J Mt Sci-Engl 17(3):556–571. https://doi.org/10.1007/s11629-019-5438-3
2. Bennett KE, Werner AT, Schnorbus M (2012) Uncertainties in Hydrologic and Climate Change Impact Analyses in Headwater Basins of British Columbia. J Clim 25(17):5711–5730. https://doi.org/10.1175/JCLI-D-11-00417.1
3. Cai D, You Q, Fraedrich K, Guan Y (2017) Spatiotemporal Temperature Variability over the Tibetan Plateau: Altitudinal Dependence Associated with the Global Warming Hiatus. J Clim 30(3):969–984. https://doi.org/10.1175/JCLI-D-16-0343.1

4. Chen C, Hsu H, Liang H (2021) Evaluation and comparison of CMIP6 and CMIP5 model performance in simulating the seasonal extreme precipitation in the Western North Pacific and East Asia. WEATHER AND CLIMATE EXTREMES 31. https://doi.org/10.1016/j.wace.2021.100303
5. Chen L, Frauenfeld OW (2014a) A comprehensive evaluation of precipitation simulations over China based on CMIP5 multimodel ensemble projections. J Geophys Res-Atmos 119(10):5767–5786. https://doi.org/10.1002/2013JD021190
6. Chen L, Frauenfeld OW (2014b) Surface Air Temperature Changes over the Twentieth and Twenty-First Centuries in China Simulated by 20 CMIP5 Models. J Clim 27(11):3920–3937. https://doi.org/10.1175/JCLI-D-13-00465.1
7. Chen S, Liu Y, Thomas A (2006) Climatic change on the Tibetan Plateau: Potential evapotranspiration trends from 1961–2000. Clim Change 76(3–4):291–319. https://doi.org/10.1007/s10584-006-9080-z
8. Chen Y, Li W, Deng H et al (2016) Changes in Central Asia's Water Tower: Past, Present and Future. Sci Rep-Uk 6. https://doi.org/10.1038/srep35458
9. Du MY, Kawashima S, Yonemura S et al (2004) Mutual influence between human activities and climate change in the Tibetan Plateau during recent years. Global Planet Change 41(3–4):241–249. https://doi.org/10.1016/j.gloplacha.2004.01.010
10. Duan A, Xiao Z (2015) Does the climate warming hiatus exist over the Tibetan Plateau? Sci Rep-Uk 5. https://doi.org/10.1038/srep13711
11. Duan J, Li L, Chen L, Zhang H (2020) Time-dependent warming amplification over the Tibetan Plateau during the past few decades. Atmos Sci Lett 21(10). https://doi.org/10.1002/asl.998
12. Eghdamirad S, Johnson F, Woldemeskel F, Sharma A (2016) Quantifying the sources of uncertainty in upper air climate variables. J Geophys Res-Atmos 121(8):3859–3874. https://doi.org/10.1002/2015JD024341
13. Eyring V, Bony S, Meehl GA et al (2016) Overview of the Coupled Model Intercomparison Project Phase 6 (CMIP6) experimental design and organization. Geosci Model Dev 9(5):1937–1958. https://doi.org/10.5194/gmd-9-1937-2016
14. Fahad MGR, Islam AKMS, Nazari R et al (2018) Regional changes of precipitation and temperature over Bangladesh using bias-corrected multi-model ensemble projections considering high-emission pathways. Int J Climatol 38(4):1634–1648. https://doi.org/10.1002/joc.5284
15. Gao X, Shi Y, Song R et al (2008) Reduction of future monsoon precipitation over China: comparison between a high resolution RCM simulation and the driving GCM. Meteorol Atmos Phys 100(1–4):73–86. https://doi.org/10.1007/s00703-008-0296-5
16. Gao Y, Chen F, Miguez-Macho G, Li X (2020) Understanding precipitation recycling over the Tibetan Plateau using tracer analysis with WRF. Clim Dynam 55(9–10):2921–2937. https://doi.org/10.1007/s00382-020-05426-9
17. Gao Y, Li X, Leung LR et al (2015) Aridity changes in the Tibetan Plateau in a warming climate. Environ Res Lett 10(3). https://doi.org/10.1088/1748-9326/10/3/034013
18. Gao Y, Xiao L, Chen D et al (2017) Quantification of the relative role of land-surface processes and large-scale forcing in dynamic downscaling over the Tibetan Plateau. Clim Dynam 48(5–6):1705–1721. https://doi.org/10.1007/s00382-016-3168-6
19. Gerber EP, Manzini E (2016) The Dynamics and Variability Model Intercomparison Project (DynVarMIP) for CMIP6: assessing the stratosphere-troposphere system. Geosci Model Dev 9(9):3413–3425. https://doi.org/10.5194/gmd-9-3413-2016
20. Gu H, Yu Z, Wang J et al (2015) Assessing CMIP5 general circulation model simulations of precipitation and temperature over China. Int J Climatol 35(9):2431–2440. https://doi.org/10.1002/joc.4152
21. Gu H, Yu Z, Yang C et al (2018) High-resolution ensemble projections and uncertainty assessment of regional climate change over China in CORDEX East Asia. Hydrol Earth Syst Sc 22(5):3087–3103. https://doi.org/10.5194/hess-22-3087-2018
22. Guo D, Pepin N, Yang K et al (2021) Local changes in snow depth dominate the evolving pattern of elevation-dependent warming on the Tibetan Plateau. Sci Bull 66(11):1146–1150. https://doi.org/10.1016/j.scib.2021.02.013
23. Guo D, Yu E, Wang H (2016) Will the Tibetan Plateau warming depend on elevation in the future? J Geophys Res-Atmos 121(8):3969–3978. https://doi.org/10.1002/2016JD024871
24. Gusain A, Ghosh S, Karmakar S (2020) Added value of CMIP6 over CMIP5 models in simulating Indian summer monsoon rainfall. Atmos Res 232. https://doi.org/10.1016/j.atmosres.2019.104680
25. Hansen J, Ruedy R, Sato M, Lo K (2010) GLOBAL SURFACE TEMPERATURE CHANGE.Rev Geophys48 (4)
26. Hawkins E, Sutton R (2011) The potential to narrow uncertainty in projections of regional precipitation change. Clim Dynam 37(1–2):407–418. https://doi.org/10.1007/s00382-010-0810-6

27. IPCC (2013) Summary for policymakers of climate change 2013: the physical science basis. Contribution of Working Group I to the fifth assessment report of the intergovernmental panel on climate change. Cambridge University Press, Cambridge
28. IPCC (2021) Summary for Policymakers. In: Climate Change 2021: The Physical Science Basis. Contribution of Working Group I to the Sixth Assessment Report of the Intergovernmental Panel on Climate Change [Masson-Delmotte, V., P. Zhai, A. Pirani, S. L. Connors, C. Péan, S. Berger, N. Caud, Y. Chen, L. Goldfarb, M. I. Gomis, M. Huang, K. Leitzell, E. Lonnoy, J.B.R. Matthews, T. K. Maycock, T. Waterfield, O. Yelekçi, R. Yu and B. Zhou (eds.)]., Cambridge University Press In Press
29. Ji Z, Kang S (2013) Projection of snow cover changes over China under RCP scenarios. Clim Dynam 41(3–4):589–600. https://doi.org/10.1007/s00382-012-1473-2
30. Jia K, Ruan Y, Yang Y, You Z (2019) Assessment of CMIP5 GCM Simulation Performance for Temperature Projection in the Tibetan Plateau. Earth Space Sci 6(12):2362–2378. https://doi.org/10.1029/2019EA000962
31. Jin X, Wu T, Li L (2013) The quasi-stationary feature of nocturnal precipitation in the Sichuan Basin and the role of the Tibetan Plateau. Clim Dynam 41(3–4):977–994. https://doi.org/10.1007/s00382-012-1521-y
32. Jobst AM, Kingston DG, Cullen NJ, Schmid J (2018) Intercomparison of different uncertainty sources in hydrological climate change projections for an alpine catchment (upper Clutha River, New Zealand). Hydrol Earth Syst Sc 22(6):3125–3142. https://doi.org/10.5194/hess-22-3125-2018
33. Kang S, Zhang Q, Qian Y et al (2019) Linking atmospheric pollution to cryospheric change in the Third Pole region: current progress and future prospects. Natl Sci Rev 6(4):796–809. https://doi.org/10.1093/nsr/nwz031
34. Kharin VV, Zwiers FW, Zhang X, Wehner M (2013) Changes in temperature and precipitation extremes in the CMIP5 ensemble. Clim Change 119(2):345–357. https://doi.org/10.1007/s10584-013-0705-8
35. Kim H, Wang B, Ding Q (2008) The Global Monsoon Variability Simulated by CMIP3 Coupled Climate Models. J Clim 21(20):5271–5294. https://doi.org/10.1175/2008JCLI2041.1
36. Kim S, Eghdamirad S, Sharma A, Kim JH (2020) Quantification of Uncertainty in Projections of Extreme Daily Precipitation. Earth Space Sci 7(8). https://doi.org/10.1029/2019EA001052
37. Kuang X, Jiao JJ (2016) Review on climate change on the Tibetan Plateau during the last half century. J Geophys Res-Atmos 121(8):3979–4007. https://doi.org/10.1002/2015JD024728
38. Li X, Wang L, Guo X, Chen D (2017) Does summer precipitation trend over and around the Tibetan Plateau depend on elevation? Int J Climatol 371:1278–1284. https://doi.org/10.1002/joc.4978
39. Liu X, Cheng Z, Yan L, Yin Z (2009) Elevation dependency of recent and future minimum surface air temperature trends in the Tibetan Plateau and its surroundings. Global Planet Change 68 (3): 164-174. https ://doi.org/10.1016/j.gloplacha.2009.03.017
40. Liu XD, Chen BD (2000) Climatic warming in the Tibetan Plateau during recent decades. Int J Climatol 20 (14): 1729-1742. https ://doi.org/10.1002/1097-0088(20001130)20:14<1729::AID-JOC556>3.0.CO;2-Y
41. Lun Y, Liu L, Cheng L et al (2021) Assessment of GCMs simulation performance for precipitation and temperature from CMIP5 to CMIP6 over the Tibetan Plateau. Int J Climatol 41(7):3994–4018. https://doi.org/10.1002/joc.7055
42. Maloney ED, Camargo SJ, Chang E et al (2014) North American Climate in CMIP5 Experiments: Part III: Assessment of Twenty-First-Century Projections*. J Clim 27(6):2230–2270. https://doi.org/10.1175/JCLI-D-13-00273.1
43. O'Neill BC, Tebaldi C, van Vuuren DP et al (2016) The Scenario Model Intercomparison Project (ScenarioMIP) for CMIP6. Geosci Model Dev 9(9):3461–3482. https://doi.org/10.5194/gmd-9-3461-2016
44. Pepin N, Bradley RS, Diaz HF et al (2015) Elevation-dependent warming in mountain regions of the world. Nat Clim Change 5(5):424–430. https://doi.org/10.1038/NCLIMATE2563
45. Prasanna V, Preethi B, Oh J et al (2020) Performance of CMIP5 atmospheric general circulation model simulations over the Asian summer monsoon region. Global Planet Change 194. https://doi.org/10.1016/j.gloplacha.2020.103298
46. Rangwala I, Miller JR, Xu M (2009) Warming in the Tibetan Plateau: Possible influences of the changes in surface water vapor. Geophys Res Lett 36. https://doi.org/10.1029/2009GL037245
47. Reichler T, Kim J (2008) How well do coupled models simulate today's climate? B Am Meteorol Soc 89(3):303. https://doi.org/10.1175/BAMS-89-3-303
48. Riahi K, van Vuuren DP, Kriegler E et al (2017) The Shared Socioeconomic Pathways and their energy, land use, and greenhouse gas emissions implications: An overview. Global Environ Chang 42:153–168. https://doi.org/10.1016/j.gloenvcha.2016.05.009

49. Rogelj J, Meinshausen M, Knutti R (2012) Global warming under old an new scenarios using IPCC climate sensitivity range estimates. Nat Clim Change 2(4):248–253. https://doi.org/10.1038/NCLIMATE1385
50. Sharma T, Vittal H, Chhabra S et al (2018) Understanding the cascade of GCM and downscaling uncertainties in hydro-climatic projections over India. Int J Climatol 381:E178–E190. https://doi.org/10.1002/joc.5361
51. Shen Y, Feng M, Zhang H, Gao F (2010) Interpolation Methods of China Daily Precipitation Data. J Appl Meteorolgical Sci 21(3):279–286
52. Song M, Wang R, Ljungqvist FC et al (2021) Winter vs. summer temperature variations on the southeastern Tibetan Plateau, 1718–2005 CE. Atmos Res 261. https://doi.org/10.1016/j.atmosres.2021.105739
53. Song YH, Chung E, Shahid S (2021) Spatiotemporal differences and uncertainties in projections of precipitation and temperature in South Korea from CMIP6 and CMIP5 general circulation models. Int J Climatol 41(13):5899–5919. https://doi.org/10.1002/joc.7159
54. Song YH, Chung E, Shiru MS (2020) Uncertainty Analysis of Monthly Precipitation in GCMs Using Multiple Bias Correction Methods under Different RCPs. Sustainability-Basel 12(18). https://doi.org/10.3390/su12187508
55. Su B, Huang J, Mondal SK et al (2021) Insight from CMIP6 SSP-RCP scenarios for future drought characteristics in China. Atmos Res 250. https://doi.org/10.1016/j.atmosres.2020.105375
56. Su F, Duan X, Chen D et al (2013) Evaluation of the Global Climate Models in the CMIP5 over the Tibetan Plateau. J Clim 26(10):3187–3208. https://doi.org/10.1175/JCLI-D-12-00321.1
57. Taylor KE (2001) Summarizing multiple aspects of model performance in a single diagram. J Geophys Res-Atmos 106(D7):7183–7192. https://doi.org/10.1029/2000JD900719
58. Taylor KE, Stouffer RJ, Meehl GA, AN OVERVIEW OF CMIP5 AND THE EXPERIMENT DESIGN (2012) B Am Meteorol Soc 93(4):485–498. https://doi.org/10.1175/BAMS-D-11-00094.1
59. Tebaldi C, Debeire K, Eyring V et al (2020) Climate model projections from the Scenario Model Intercomparison Project (ScenarioMIP) of CMIP6
60. Thakuri S, Dahal S, Shrestha D et al (2019) Elevation-dependent warming of maximum air temperature in Nepal during 1976–2015. Atmos Res 228:261–269. https://doi.org/10.1016/j.atmosres.2019.06.006
61. Tokarska KB, Stolpe MB, Sippel S et al (2020) Past warming trend constrains future warming in CMIP6 models. Sci Adv 6(12). https://doi.org/10.1126/sciadv.aaz9549
62. Wang B, Biasutti M, Byrne MP et al (2021) Monsoons Climate Change Assessment. B Am Meteorol Soc 102(1):E1–E19. https://doi.org/10.1175/BAMS-D-19-0335.1
63. Wang Q, Fan X, Wang M (2021) Warming amplification with both altitude and latitude in the Tibetan Plateau. Int J Climatol. https://doi.org/10.1002/joc.7418
64. Wang X, Yang T, Wortmann M et al (2017) Analysis of multi-dimensional hydrological alterations under climate change for four major river basins in different climate zones. Clim Change 141(3):483–498. https://doi.org/10.1007/s10584-016-1843-6
65. Watterson IG (2015) Improved Simulation of Regional Climate by Global Models with Higher Resolution: Skill Scores Correlated with Grid Length*. J Clim 28(15):5985–6000. https://doi.org/10.1175/JCLI-D-14-00702.1
66. Woldemeskel FM, Sharma A, Sivakumar B, Mehrotra R (2012) An error estimation method for precipitation and temperature projections for future climates. J Geophys Res-Atmos 117. https://doi.org/10.1029/2012JD018062
67. Woldemeskel FM, Sharma A, Sivakumar B, Mehrotra R (2014) A framework to quantify GCM uncertainties for use in impact assessment studies. J Hydrol 519:1453–1465
68. Woldemeskel FM, Sharma A, Sivakumar B, Mehrotra R (2016) Quantification of precipitation and temperature uncertainties simulated by CMIP3 and CMIP5 models. J Geophys Res-Atmos 121(1):3–17. https://doi.org/10.1002/2015JD023719
69. Wu T, Yu R, Lu Y et al (2021) BCC-CSM2-HR: a high-resolution version of the Beijing Climate Center Climate System Model. Geosci Model Dev 14(5):2977–3006. https://doi.org/10.5194/gmd-14-2977-2021
70. Yang Q, Yu Z, Wei J et al (2021) Performance of the WRF model in simulating intense precipitation events over the Hanjiang River Basin, China - A multi-physics ensemble approach. Atmos Res 248. https://doi.org/10.1016/j.atmosres.2020.105206
71. Yao T, Thompson L, Yang W (2012) Different glacier status with atmospheric circulations in Tibetan Plateau and surroundings. Nat Clim Change 2:663–667. https://doi.org/10.1038/nclimate1580

72. Yao T, Xue Y, Chen D et al (2019) Recent Third Pole's Rapid Warming Accompanies Cryospheric Melt and Water Cycle Intensification and Interactions between Monsoon and Environment: Multidisciplinary Approach with Observations, Modeling, and Analysis. B Am Meteorol Soc 100(3):423–444. https://doi.org/10.1175/BAMS-D-17-0057.1
73. Yip S, Ferro CAT, Stephenson DB, Hawkins E (2011) A Simple, Coherent Framework for Partitioning Uncertainty in Climate Predictions. J Clim 24(17):4634–4643. https://doi.org/10.1175/2011JCLI4085.1
74. You Q, Cai Z, Wu F et al (2021) Temperature dataset of CMIP6 models over China: evaluation, trend and uncertainty. Clim Dynam 57(1–2):17–35. https://doi.org/10.1007/s00382-021-05691-2
75. You Q, Chen D, Wu F et al (2020) Elevation dependent warming over the Tibetan Plateau: Patterns, mechanisms and perspectives. Earth-Sci Rev 210. https://doi.org/10.1016/j.earscirev.2020.103349
76. You Q, Zhang Y, Xie X, Wu F (2019) Robust elevation dependency warming over the Tibetan Plateau under global warming of 1.5 degrees C and 2 degrees C. Clim Dynam 53(3–4):2047–2060. https://doi.org/10.1007/s00382-019-04775-4
77. Zamani Y, Monfared SAH, Moghaddam MA, Hamidianpour M (2020) A comparison of CMIP6 and CMIP5 projections for precipitation to observational data: the case of Northeastern Iran. Theor Appl Climatol 142:3–4
78. Zhang QB, Cheng GD, Yao TD et al (2003) A 2,326-year tree-ring record of climate variability on the northeastern Qinghai-Tibetan Plateau. Geophys Res Lett 30(14). https://doi.org/10.1029/2003GL017425
79. Zhao F, He M, Wang Y et al (2022) Eco-geological environment quality assessment based on multi-source data of the mining city in red soil hilly region, China. J Mt Sci-Engl 19(1):253–275. https://doi.org/10.1007/s11629-021-6860-x
80. Zhou T (2021) New physical science behind climate change: What does IPCC AR6 tell us? Innovation (N Y) 2. 100173. https://doi.org/10.1016/j.xinn.2021.100173. 4
81. Zhou T, Chen X, Wu B et al (2017) A Robustness Analysis of CMIP5 Models over the East Asia-Western North Pacific Domain. Engineering-Prc 3(5):773–778. https://doi.org/10.1016/J.ENG.2017.05.018
82. Zhou T, Chen Z, Zou L et al (2020) Development of Climate and Earth System Models in China: Past Achievements and New CMIP6 Results. J Meteorol Res-Prc 34(1):1–19. https://doi.org/10.1007/s13351-020-9164-0
83. Zhou T, Yu R (2006) Twentieth-century surface air temperature over China and the globe simulated by coupled climate models. J Clim 19(22):5843–5858. https://doi.org/10.1175/JCLI3952.1
84. Zhu H, Jiang Z, Li L (2021) Projection of climate extremes in China, an incremental exercise from CMIP5 to CMIP6. Sci Bull 66(24):2528–2537. https://doi.org/10.1016/j.scib.2021.07.026
85. Zhu Y, Yang S (2020) Evaluation of CMIP6 for historical temperature and precipitation over the Tibetan Plateau and its comparison with CMIP5. ADVANCES IN CLIMATE CHANGE RESEARCH 11. 239–251. https://doi.org/10.1016/j.accre.2020.08.001. 3
86. Zou H, Zhu J, Zhou L et al (2014) Validation and Application of Reanalysis Temperature Data over the Tibetan Plateau. J Meteorol Res-Prc 28(1):139–149. https://doi.org/10.1007/s13351-014-3027-5

Figures

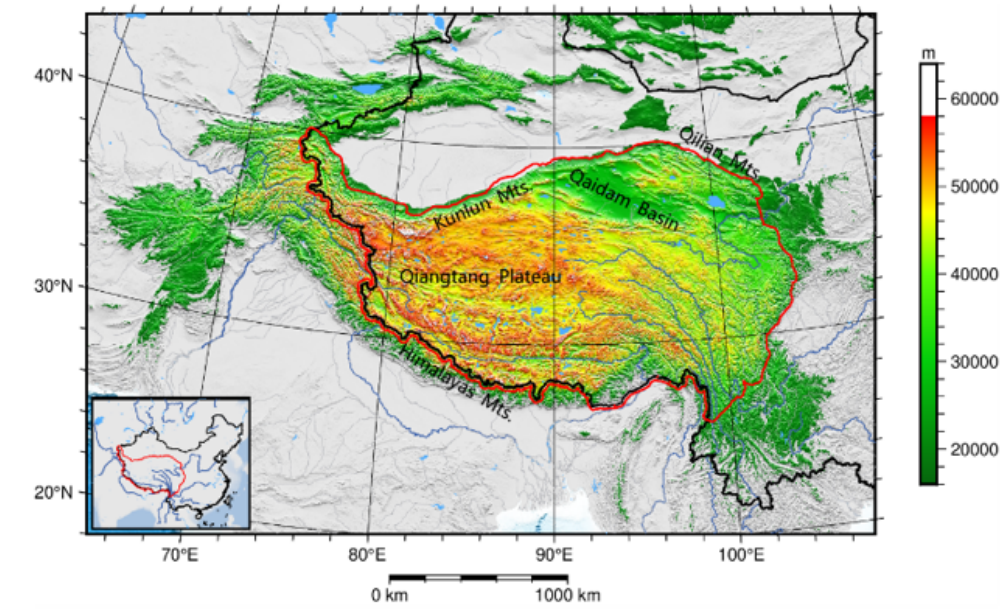

Figure 1

Topography of the Tibetan Plateau (TP) in this study. The red line is the contour of the TP

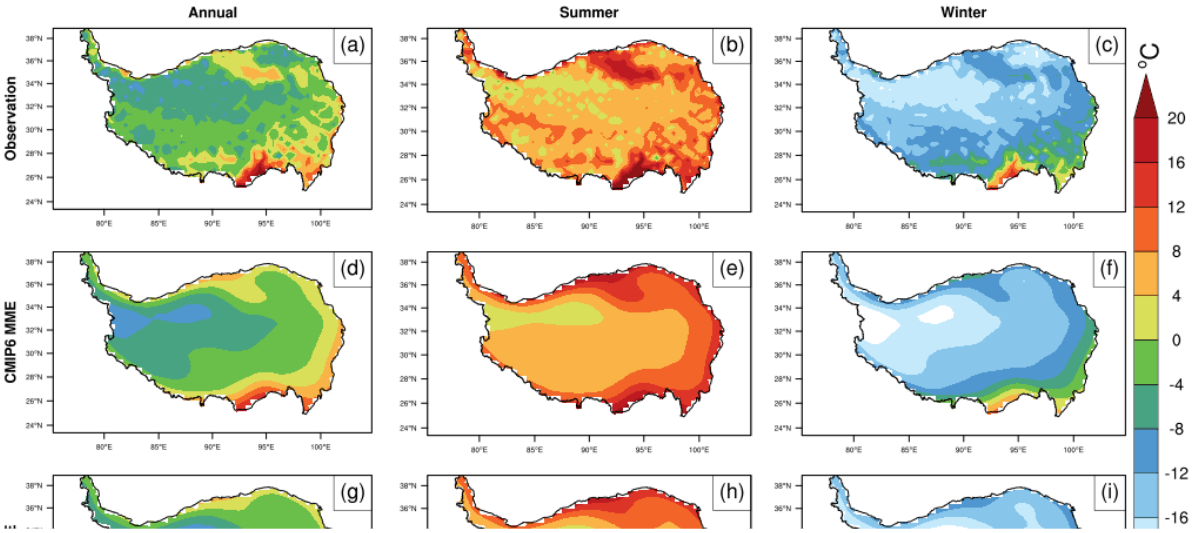

Figure 2

The spatial distribution of the average annual (left column), summer (JJA, middle column) and winter (DJF, right column) surface mean temperature during 1961-2005 from the observations (the first line), CMIP6 model historical run (the second line), CMIP5 model historical run (the third line), and the relative differences between the observation (the fourth and fifth lines). The multi-model ensemble (MME) means of 14 CMIP5 models and 14 CMIP6 models are calculated over the Tibetan Plateau

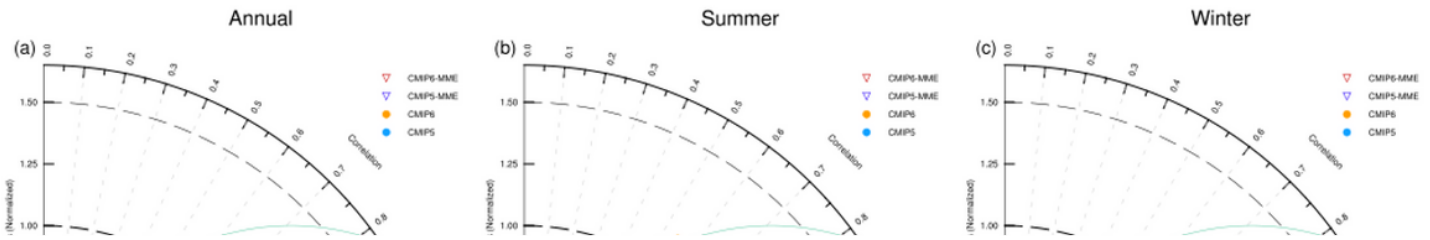

Figure 3

Taylor diagrams showing correlation coefficients, standard deviations, and root mean square errors (RMSE) between observed and simulated annual (a), summer (b) and winter (c) surface mean temperature from CMIP5 and CMIP6 over the TP during 1961-2005. The MME refers to a combination of 14 CMIP5/6 models

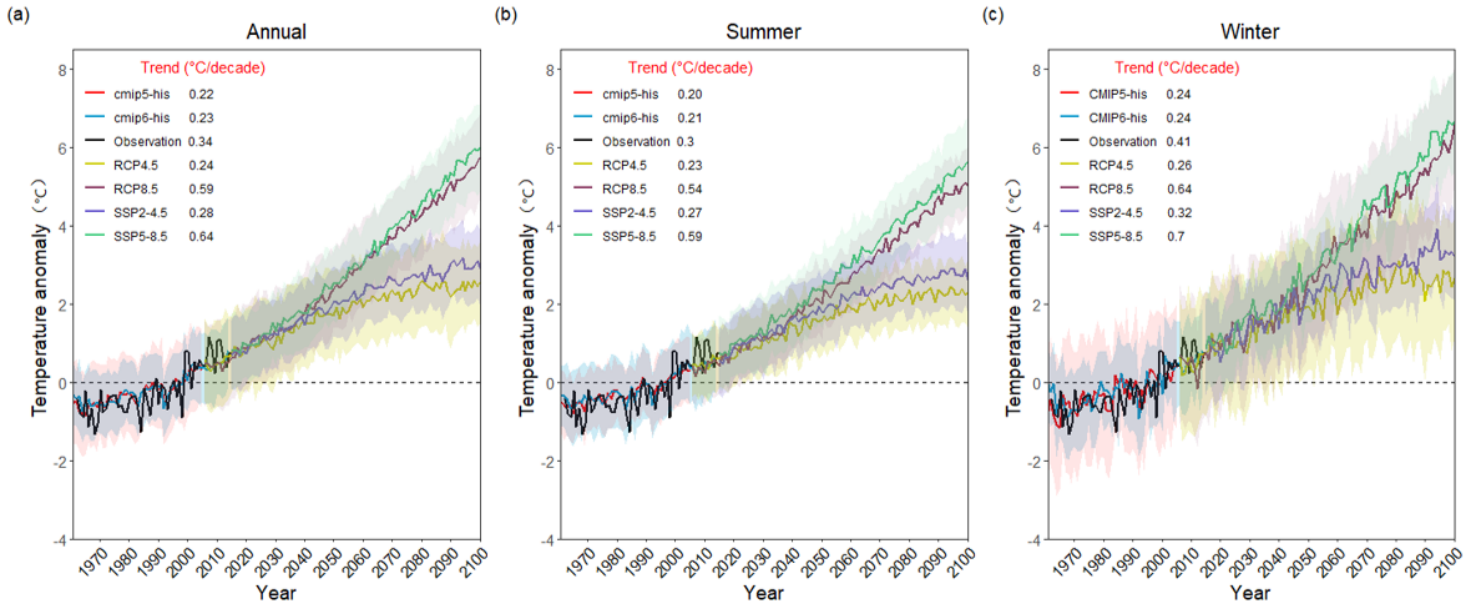

Figure 4

Time series of annual (a), summer (b) and winter (c) surface mean temperature anomalies during 1961-2100 (relative to 1986-2005) over the Tibetan Plateau for the observations, historical simulations and future projections from the MMEs of CMIP5 and CMIP6 models. The shadings denote the 95 model intervals (The warming rates are calculated for the observations and CMIP5/6 historical run during 1961-2005, for RCP and SSP scenarios during 2015-2100, respectively.)

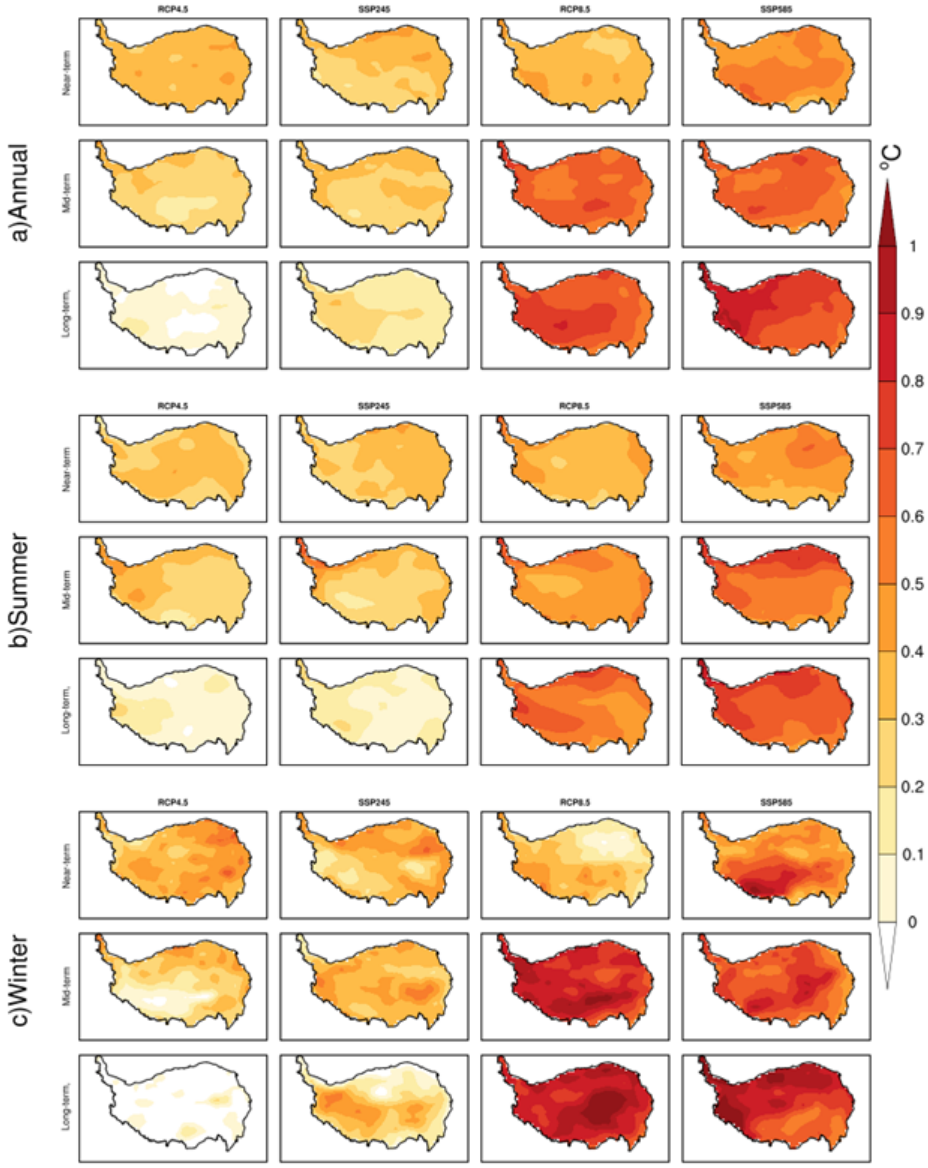

Figure 5

Spatial distribution of annual (a), summer (b) and winter (c) surface mean temperature from the MME of CMIP5 and CMIP6 over the TP under two RCP and two SSP scenarios during three future periods relative to the period of 1986–2005

Figure 6

As in Fig.5, but for warming trends of surface mean temperature (°C/decade)

Figure 7

Range of projected changes in annual (left column), summer (middle column) and winter (right column) surface air temperature relative to 1986-2005 period from the MMEs of CMIP5/6 under RCP4.5, RCP8.5, SSP2-4.5 and SSP5-8.5 scenarios with increasing elevation on the TP in the near-term (2021-2040), mid-term (2041-2060) and long-term (2081-2100). The box plots indicate the 10th and 90th percentiles (solid bars of the box ends), median (black dots) and mean (red bars)

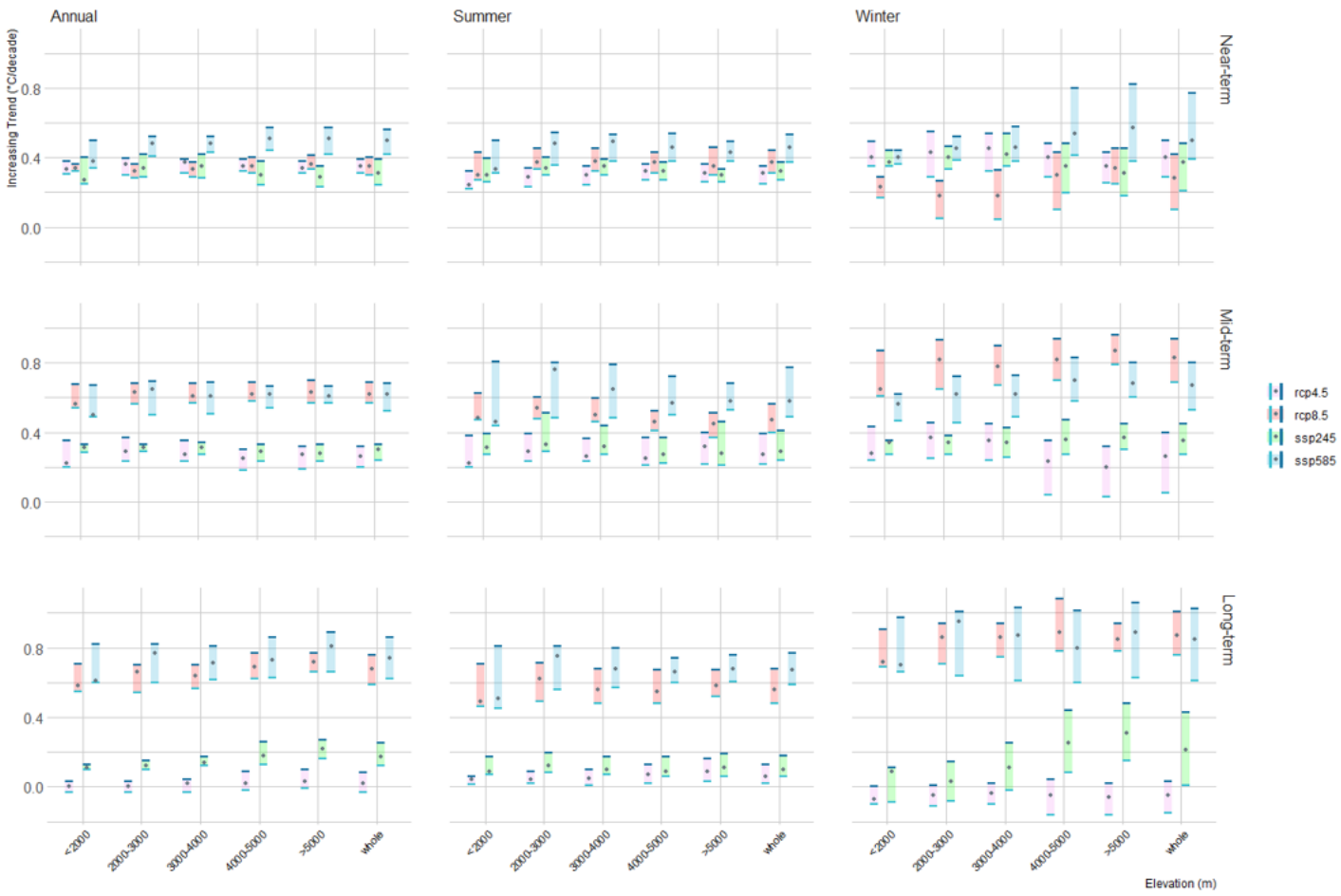

Figure 8

As in Fig.7, but for warming trends of surface mean temperature (°C/decade)

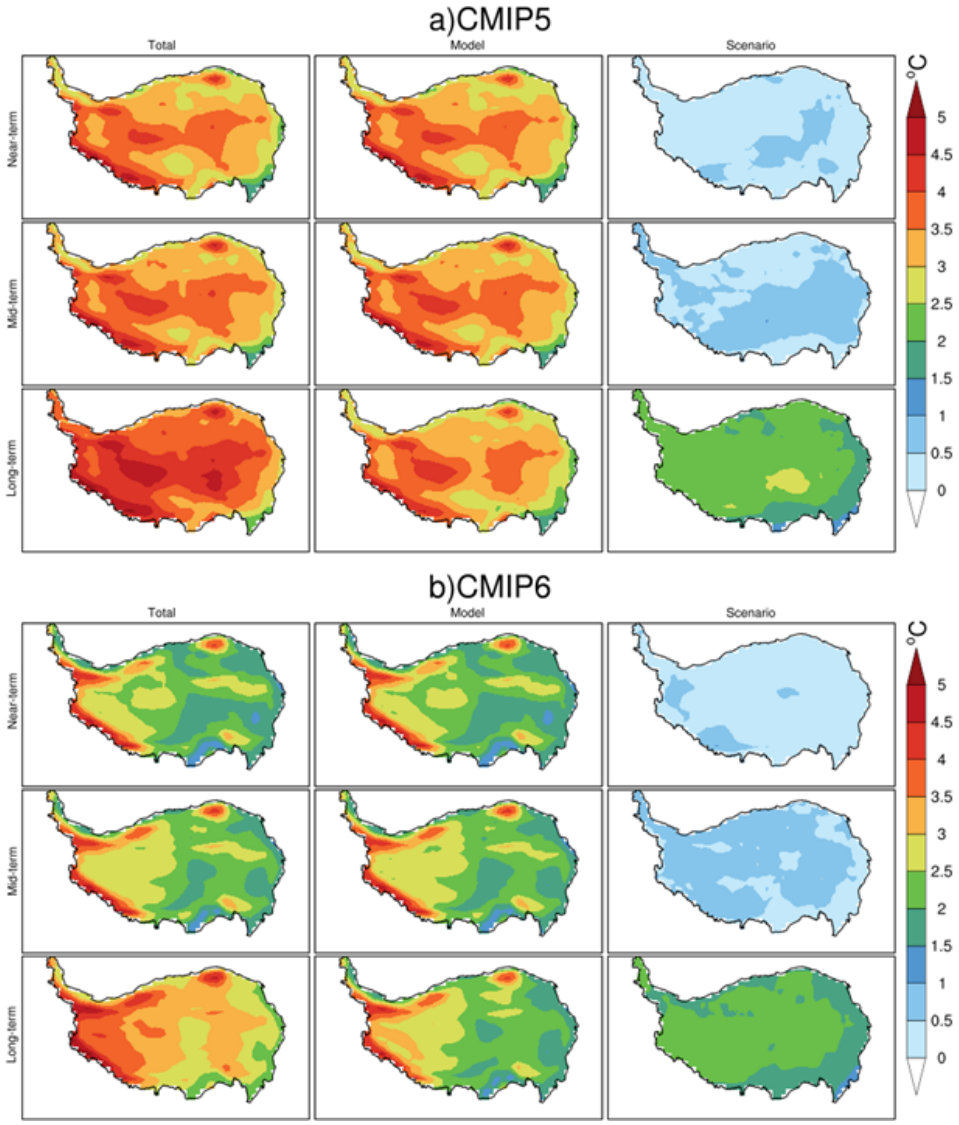

Figure 9

Spatial distribution of square root error variance (SREV) values of annual surface mean temperature for total, model and scenario uncertainty from CMIP5 (a) and CMIP6 (b) in the near-term (2021-2040), mid-term (2041-2060) and long-term (2081-2100)

Figure 10

Range of SREV values of annual surface mean temperature for total, model and scenario uncertainty from CMIP5/6 with increasing elevation over the Tibetan Plateau in the near-term (2021-2040), mid-term (2041-2060) and long-term (2081-2100). The violin plots represent the distribution of the data, and the box plots indicate the 25th and 75th percentiles (endpoints of the line segment) and mean (black dots)

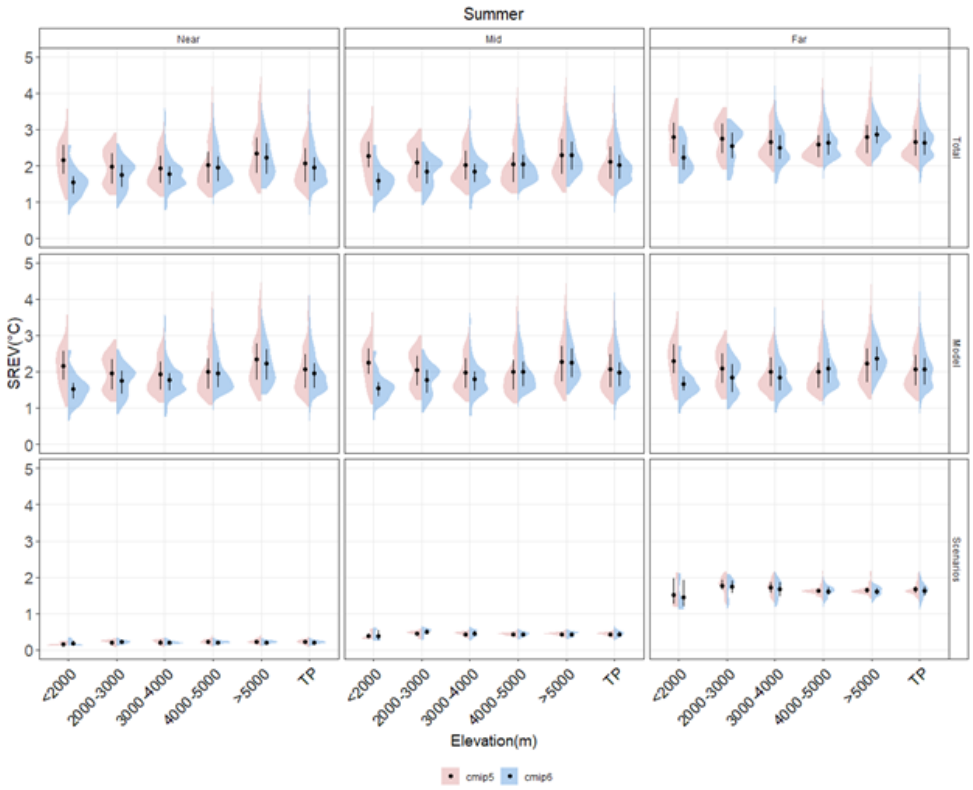

Figure 11

As in Fig.10, but for SREV values of summer surface mean temperature

Figure 12

As in Fig.10, but for SREV values of winter surface mean temperature